
Supporting Information

Generation, characterization, and application of hierarchically structured self-assembly induced by the combined effect of self-emulsification and phase separation

Xiuyu Wang, Yi Hou, Li Yao,* Mingyuan Gao,* Maofa Ge

Beijing National Laboratory for Molecular Science, Institute of Chemistry, Chinese Academy of Sciences, Beijing 100190, China

* To whom correspondence should be addressed.

E-mail: yaoli@iccas.ac.cn; gaomy@iccas.ac.cn

Experimental Section

Chemicals and reagents

Ferric acetylacetonate ($\text{Fe}(\text{acac})_3$), oleic acid (OA), oleylamine, phenyl ether, 1,2-hexadecanediol, *N,N*-dicyclohexylcarbodiimide (DCC), *N*-hydroxysuccinimide (NHS) and dopamine hydrochloride were purchased from Aladdin and used as received. Polyethylene glycol (PEG, $M_w \approx 6000$) and polyethylene glycol diacid ($M_w \approx 600$) were provided by Sigma-Aldrich. Fluorescein, lauric acid and polystyrene (PS, $M_w \approx 6000$) were obtained from J&K. Other chemicals of analytical grade including ethanol, dichloromethane, tetrahydrofuran (THF), dimethyl formamide (DMF), sodium carbonate (Na_2CO_3) and sodium dodecyl sulfate (SDS) were used as received.

Synthesis of oil dispersed Fe_3O_4 nanoparticles

Fe_3O_4 nanoparticles of about 5 nm in diameter were synthesized following the procedure previously reported in the literature.¹ Generally, a mixture of $\text{Fe}(\text{acac})_3$ (2 mmol), phenyl ether (20 mL), oleic acid (6 mmol), oleylamine (6 mmol) and 1,2-hexadecanediol (15 mmol) was magnetically stirred under a flow of nitrogen. The

mixture was heated to 200 °C for 30 min and then refluxed at 265 °C for another 30 min by the protection of nitrogen. After cooled to room temperature, the black product was precipitated from the solution by ethanol. The resultant nanoparticles were washed with ethanol for three times, and finally were redispersed in dichloromethane for further experiments.

Preparation of water-soluble Fe₃O₄ nanoparticles via ligand exchange

For the biomedical applications, individual Fe₃O₄ nanoparticles need to be converted to aqueous dispersion by ligands exchange with PEG. According to the reported method, PEG modified Fe₃O₄ magnetic nanoparticles were obtained through a general ligand exchange procedure.² As a typical example, PEG diacid (20 mg), NHS (2 mg), DCC (3 mg) and dopamine hydrochloride (1.27 mg) were dissolved in a mixture solvent containing CHCl₃ (2 mL), DMF (1 mL), and anhydrous Na₂CO₃ (10 mg). The solution was stirred at room temperature for 2 h. Then Fe₃O₄ nanoparticles (5 mg) were added, the reaction mixture was stirred overnight at room temperature under N₂ protection. Finally, the black sediments were obtained after treating with hexane, and dried under vacuum at room temperature. The final powders were readily dissolved in water, supporting that the PEG coating was effectively realized.³

Synthesis of MSHS

The hierarchically structured magnetic single-hole hollow spheres (MSHS) were produced through three major stages: single emulsions → double emulsions → self-assembly. This process depends on a controlled fabrication of monodispersed single droplets at the first stage, which has been realized through a microfluidics

device. In a typical procedure, the dispersed organic phase was 0.9 mg/mL Fe₃O₄ nanoparticles and PEG 6000 with varying concentration in dichloromethane. The aqueous solution with 0.25 % SDS as a surfactant to stabilize the droplets was served as the continuous aqueous phase. When the two phases were injected into the microfluidics device which consists of a tapered glass capillary nested inside an around one to form a coaxial geometry, the dispersed phase was sheath by the continuous flow at the exit orifice to form uniform single droplets. These starting single emulsions were collected by a petri dish under a saturated dichloromethane vapor atmosphere, and then were transferred into a refrigerator at relatively low temperature (2 °C) for 40 min. Afterwards, monodispersed double emulsions with a core-shell structure could then be obtained from the morphological transformation of the starting droplets. After formation of the double emulsions, dichloromethane was allowed to evaporate into the surrounding air at 15 °C for 12 h in order to further solidify the as-synthesized double emulsions. Then, the solidified product was collected by a permanent magnet. Finally, the samples were ultrasonically washed in water for three times and the final solution was then dialyzed against water for 2 days to completely remove residual SDS. After that aqueous individually dispersed hollow spheres could be obtained. Highly uniform samples could be achieved by gradient centrifugation.

Characterization of Materials

All transmission electron microscopic (TEM) images of the primary OA coated magnetic nanoparticles (OA-Fe₃O₄) and the hierarchical assemblies were obtained

using a JEM-2011 microscope at an accelerating voltage of 200 kV. To prepare TEM sample, a drop of aqueous solution of MSHS was dripped on the surface of a carbon-coated copper grid in the presence of a magnetizing field. The solvent was allowed to evaporate within 20 min. Thin sections of MSHS were obtained at room temperature using a Leica Ultracut UCT equipped with a glass knife and were collected on carbon coated TEM grids. Scanning electron microscopy (SEM) images were taken on a JEOL JSM-6700F scanning electron microscope at an accelerating voltage of 150 kV. Before imaging, the SEM samples were coated with a thin layer of gold (15 nm). Atomic force microscopy (AFM) images were acquired using a Nanoscope IIIa AFM in tapping mode. The samples were prepared by dripping the as-prepared MSHS-400 suspension onto a new cleaved mica and drying at room temperature for 24 h before measurements. Small-angle X-ray scattering (SAXS) measurements were performed on a Nanostar U small-angle X-ray scattering system using Cu K α radiation ($\lambda_{\text{CuK}\alpha} = 1.5418 \text{ \AA}$). The SAXS data at room temperature were collected over a 2θ scattering range $0.5 - 2.8^\circ$ with a step 0.02. Dynamic light scattering (DLS) was measured in water with a Nicomp 380 DLS. The iron contents of the prepared particles were determined by the colorimetric method using *o*-phenanthroline.⁴ Confocal laser scanning microscopy (CLSM) images were obtained using a Carl Zeiss LSM 510 META confocal microscope with an excitation wavelength of 480 nm. To visualize the formation of double emulsions, fluorescein, an oil-soluble green fluorescent dye was added in the dispersed phase to trace the structural evolution of single droplets. The magnetic properties of all the samples

were measured using vibrating sample magnetometer (VSM) and quantum superconducting quantum interference device (SQUID). VSM data were collected on the BKY-400 magnetometer with a sensitivity of 2×10^{-5} emu. SQUID magnetometry was performed using a Quantum Design MPMS with dc detection from Oxford Instruments. From the measured T_B , the magnetic anisotropy constant is calculated by the equation $K = 25k_B T_B / V$, where k_B is Boltzmann's constant and V is the volume of a single Fe_3O_4 nanoparticle.⁵ The magnetic remanence was obtained by a homemade atomic magnetometer with the sensitivity of $200 \text{ fT}/(\text{Hz})^{1/2}$. For the preparation of magnetic remanence samples, 25 μg of the as-prepared MSHS was placed on a sample holder, which was located 15 mm from the atomic detector. Prior to the measurements, the samples were magnetized by approaching the pole face of a permanent magnet vertically. The T_2 -weighted MR images were acquired on a 3 T clinical MRI instrument (GE signa 3.0T HD, Milwaukee, WI). The parameters for T_2 measurements were set as follows: TR = 2000 ms, and TE = 20, 40, 60, 80, 100 ms, respectively. The PEG/ Fe_3O_4 mass ratio was calculated through thermogravimetric analysis (TGA, TA-Q500 instrument). The heating rate was $10 \text{ }^\circ\text{C} \cdot \text{min}^{-1}$, and the experiments were performed in a continuous nitrogen flow at a flow rate of $20 \text{ mL} \cdot \text{min}^{-1}$. The temperature was ranged from 25 to $700 \text{ }^\circ\text{C}$. The thermostability of the MSHS was investigated by using differential scanning calorimetry (DSC, TA-Q2000 instrument). Heating scans were performed at a rate of $10 \text{ }^\circ\text{C} \cdot \text{min}^{-1}$ in a continuous nitrogen flow rate of $50 \text{ mL} \cdot \text{min}^{-1}$ and the measurements were taken between 20 and $180 \text{ }^\circ\text{C}$.

BAS loading

In this paper, MSHS-150 was used representatively for the remaining experiments. MSHS-150 was collected by a permanent magnet and then dried under a clean and slightly vacuum environment at 37 °C for 3 days. Then, MSHS-150 in dry state of 5.0 mg was mixed with 2.0 mL of PBS solution containing 20 mg of BSA. The resulting suspension was stirring gently at 37 °C for 24 h to absorb the BSA. The MSHS-150 with BSA loaded (64.6 mg/g), which was designated as MSHS-150 (BSA), was then separated from the mixture solution by a magnet.

Capping the holes on the MSHS-150(BSA) surface with phase change material (PCM)

First, a lauric acid solution in ethanol (8 wt%) was spin-coated on Si substrate at 3000 rpm for 30 s and a PCM film was obtained with a thickness of 60 nm. 10 µL of the suspension of as-obtained MSHS-150 (BSA) in water and isopropanol mixture (v/v=1:2) was carefully dripped on an elastic PDMS substrate (0.5 cm × 0.5 cm × 0.5 cm) in the presence of a static magnetizing field. The resultant PCM film was then brought into contact with the MSHS-150(BSA) supported on the PDMS substrate. A soft press is given to push the MSHS-150(BSA) partially into the PCM film. The good flexibility led to a conformal contact between the particles and the PCM film, achieving essentially 100% capping. After that, the sample was exposed to ethanol vapor for 3 min and then placed in a vacuum-chamber. Exposure of the sample to ethanol vapor allowed a viscous flow for the PCM, which could seal the holes under a vacuum state. The PCM capped MSHS-150 was then peeled off from the PDMS

substrate by holding it in an ultrasonic bath for 15 s. The ultrasonication was conducted in an ice water bath to prevent undesired melting of the PCM corks. Finally, these samples were collected by a magnet and redispersed in PBS for the next release experiment.

Magnetic field triggered release of BSA

After the capping process with PCM, the residual BSA without encapsulation in the MSHS-150 was removed by washing several times with PBS. The BSA-loaded particles were immersed in 5 mL of PBS and the suspension was gently stirred at room temperature for 5 h. Then the suspension was placed inside a water-cooled copper coil which produces a high-frequency magnetic field (500 kHz at 37.3 kA m). The external field was turned on for 5 min and then removed. Afterwards the sample solution was removed from the magnetic field and was gently stirred at room temperature for 12 h. Then another magnetic stimuli of 5 min was applied, triggering a secondary release of residual BSA. The medium solution was collected and replaced with fresh buffer in different time, especially after each period of magnetic stimulation. The cumulative release study of BSA was analyzed by measuring the concentration of released BSA in the extracted supernatant using the BCA assay.⁶

Magnetic-guided transport

To demonstrate the magnetic manipulation of the MSHS, we created an aqueous droplet of around 300 μm diameter, containing the MSHS-150 inside a mixture of 50% glycerol and 50% water (w/w, $\eta \approx 1.18 \text{ g/cm}^3$). MSHS-150 were magnetically manipulated inside the confined environment of the droplet using a simple magnet

(Neodymium Iron Boron, 4 cm × 1 cm × 0.5 cm), which generates a field of ~ 0.2 T at the ends of the poles. The magnet was placed at 1 mm from the droplet edge, in the three different directions, namely 1, 2, and 3, respectively, to manipulate the movement of MSHS. A control experiment was also executed for the free 5-nm MNPs under the same experimental conditions. The process was monitoring by a microscope tracking device consisting of an inverted microscope (OLYMPUS IX70). Particle positions were determined by means of a tracking software, and then the particle velocities along a fixed magnetic direction were calculated. The associated forces were finally determined using Stokes' law: $F = 6\pi\eta rv$, where η is medium viscosity, r is the particle's radius, and v is the velocity of the particles.⁷

Additional Characterization Data

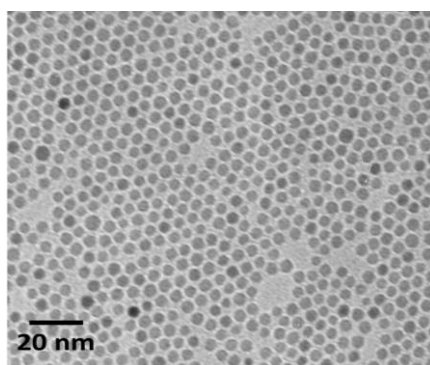


Figure S1. TEM image of individual OA-coated Fe₃O₄ nanoparticles.

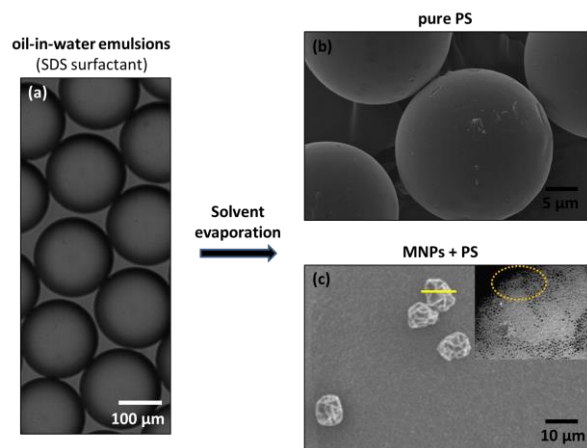


Figure S2. Control experiment confirmed that MNPs play a crucial role in generating an uneven distribution of interfacial tension. (a) Optical microscopy image showing emulsion droplets. Monodisperse emulsion droplets were generated through a microfluidics device. The organic phase consists of polystyrene (PS, $M_w \approx 6000$) with or without MNPs in dichloromethane, and aqueous phase consists of 0.25wt% sodium dodecyl sulfate (SDS). (b) SEM images of PS particles without MNPs. (c) SEM images of PS particles including 5 nm size MNPs (feed volume fraction of MNPs (ϕ_{MNPs}) = 0.02)). The inset in (c) is TEM images of a thin particle cross-section, showing the spatial distribution of MNPs. MNPs that locate in the interface of particles were indicated by a yellow dashed circle. The spherical PS particles were formed because of isotropic interfacial tension at the emulsion surface. On the contrary, the addition of a small amount of MNPs led to an interesting change in the overall shape of the PS particles from spherical to an irregular shape. The results suggest that the MNPs can be effective surfactants for producing an uneven distribution of interfacial tension, driven by their quasi-irreversible adsorption to the interface of droplets.⁸

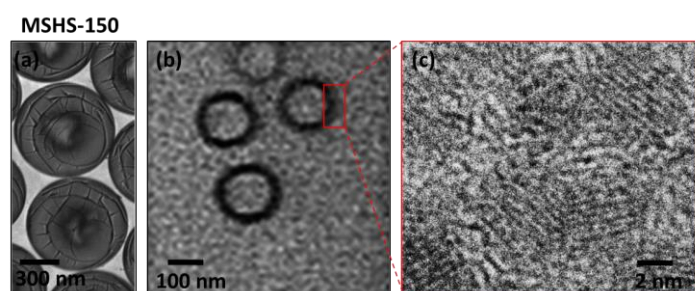


Figure S3. Typical TEM (a), XTEM (b) and HR-TEM (c) of MSHS-150. The red box is indicating the HR-TEM image of the area.

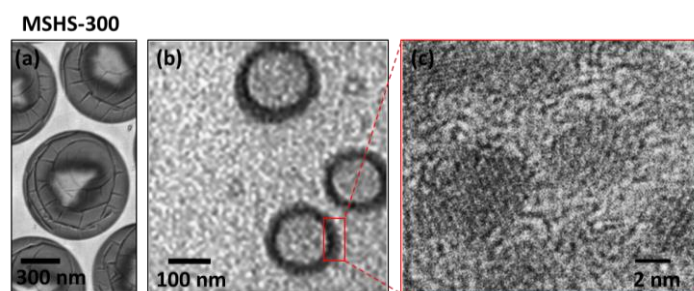


Figure S4. Typical TEM (a), XTEM (b) and HR-TEM (c) of MSHS-300. The red box is indicating the HR-TEM image of the area. The results show that the three samples (MSHS-150, 300 and 400) have the same thickness.

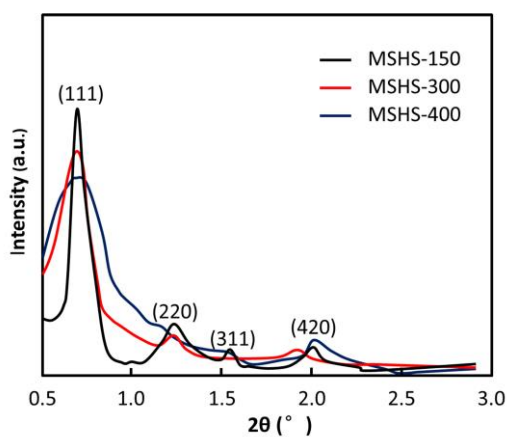


Figure S5. SAXS patterns of MSHS.

Small-angle X-ray scattering (SAXS) measurements were performed to obtain detailed information about the shell structure of the MSHS. The SAXS pattern of MSHS-150 exhibits four scattering peaks, which can be assigned to the 111, 220, 311, 420 reflections of a face centered cubic (fcc) structure (the black curve), indicating the high ordering of the shell structure.⁹ Upon the hole size increasing, the intensity of diffraction peaks decreases. For MSHS-400, the 3rd order diffraction almost disappears, suggesting the order of self-assemble structures decreases with an increase of the hole size.

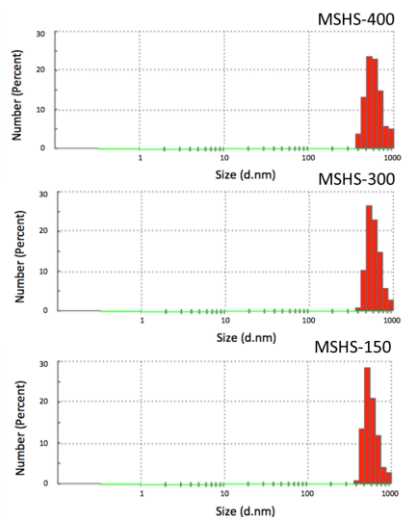


Figure S6. Dynamic light scattering (DLS) measurements of MSHS (Hydrodynamic (HD) size measurements). The diameter of the samples obtained by TEM measurement shown in Figure 2 of the main text is ~ 650 nm. The increased size is due to the hydration layer formed by the water soluble PEG.

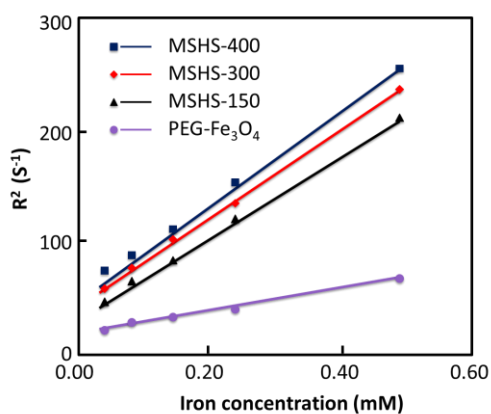


Figure S7. Transverse relaxivity coefficients (R_2) of MSHS and individual PEG-coated Fe_3O_4 nanoparticles at different concentrations in water.

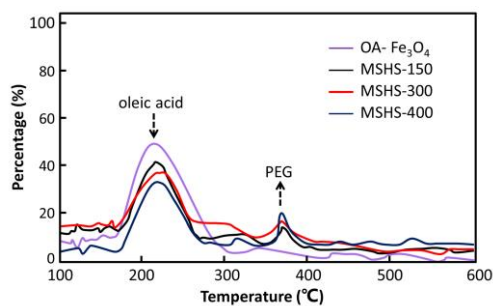


Figure S8. TGA weight loss curves of OA coated Fe_3O_4 and MSHS.

Thermogravimetric analysis (TGA) was used to calculate the PEG/ Fe_3O_4 mass ratio in the MSHS system since the PEG concentration is relevant with surface hydrophilicity. To avoid the influence of the SDS on value of the weight loss, the MSHS samples were dialyzed against water and ethanol to completely remove the SDS before the TGA testing. In the TGA analysis, the first mass loss of 50 wt% at around 230 °C is attributed to the mass loss of oleic acid, so the mass percentage of OA in the initial magnetic nanoparticles is about 50%. Comparing with the TGA of the individual Fe_3O_4 nanoparticles, one can see that the OA content decreased after the self-assembly processing. This implied that density of the organic coating round the nanoparticles decreased after the formation of MSHS. From the second weight loss at 410 °C, the PEG content was evaluated to be 6.6 wt%, 7.2 wt% and 9.6 wt% for the MSHS-150, MSHS-300 and MSHS-400, respectively. Thus the PEG content increased with increasing amount in the feed solution utilized in the synthesis of MSHS. However, comparing with the initial weight ratio, the corresponding residual PEG content decreased after the generating of MSHS because the PEG concentration can be changed in the self-emulsification procedure. From the two weight loss, the magnetic nanoparticles content was evaluated to be 52wt%, 54 wt%, 59 wt% for the

MSHS-150, MSHS-300 and MSHS-400 respectively. Thus the PEG/Fe₃O₄ mass ratio for the MSHS-150, MSHS-300 and MSHS-400 is 12.7%, 13.9% and 16.3%, respectively.

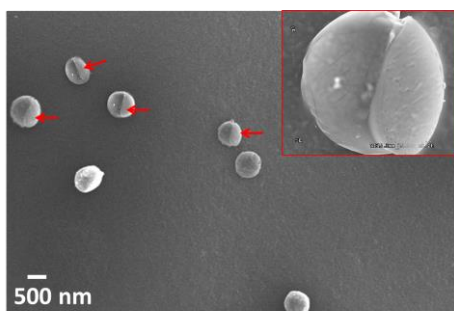


Figure S9. SEM image of MSHS-150 capped with a heat-sensitive phase change materials

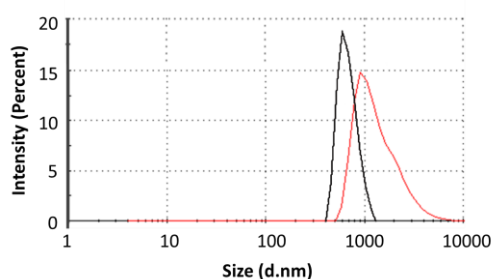


Figure S10. DLS data of MSHS-150 in different time at room temperature. The black and red lines represent freshly prepared and six-month-old samples, respectively.

In order to investigate the long term stability of MSHS in aqueous solution, DLS data in different time were provided. Compared with a freshly prepared sample, coalesced MSHS-150 were observed after six months of fabrication, which indicates a

progressive desorption PEG molecules from the shell surfaces by aging.

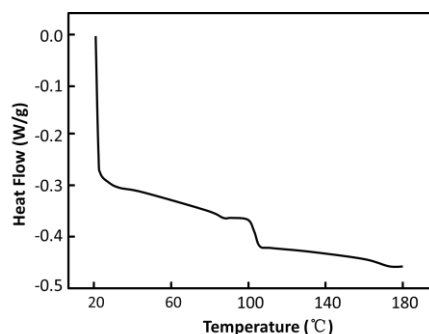


Figure S11. DSC data of MSHS-150.

Figure S11 shows the DSC thermogram of MSHS-150, based on which the thermostability can be reflected from the aspects of the endothermic peak observed at 103 °C. This suggests that the shell structure of MSHS-150 should be stable in heat generation process because the endothermic point is much higher than the phase change temperature of PCM (43 °C).

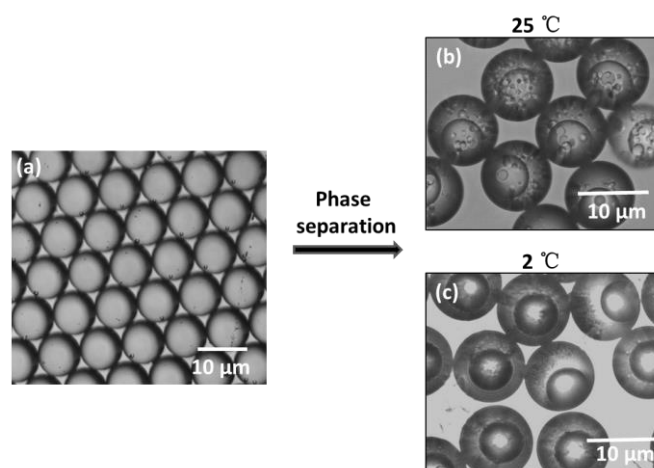


Figure S12. (a) Optical microscopy image showing monodisperse oil-in-water droplets generated through a microfluidics device. The organic dispersed phase consists of PEG and MNPs in dichloromethane, and the continuous phase is the aqueous phase of SDS solution. When the preformed droplets were kept under a saturated dichloromethane vapor atmosphere at room temperature, double emulsions with lame phase separation formed after 40 min. However, when the preformed droplets were kept under a saturated dichloromethane vapor atmosphere at a relatively low temperature (2 °C), well-defined double emulsions were produced. The results

showed that the setting temperature can be relevant with the degree of phase separation.

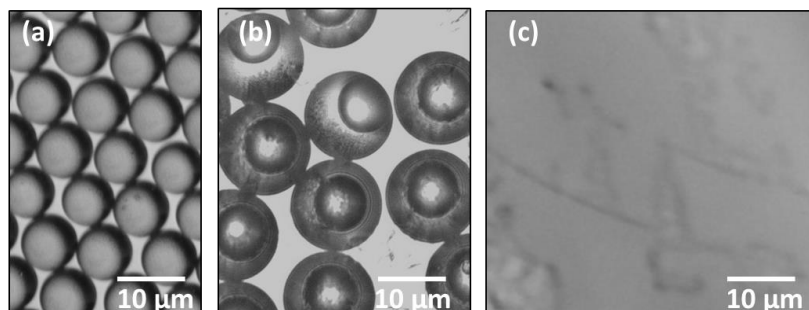


Figure S13. (a) Optical microscopy image showing monodisperse oil-in-water droplets generated through a microfluidics device. The organic dispersed phase consists of PEG in dichloromethane, and the continuous phase is the aqueous phase of SDS solution. The preformed droplets were kept under a saturated dichloromethane vapor atmosphere at a relatively low temperature (2 °C). Interestingly, double emulsions formed after 40 min due to diffusion-induced phase separation (b). However, in the absence of MNPs, the double emulsions underwent instability and disappeared quickly in the continuous phase, suggesting that MNPs is critical to stabilizing the double emulsion during solvent evaporation.

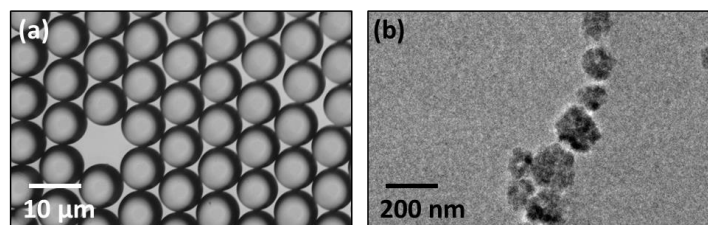


Figure S14. (a) Optical microscopy image showing monodisperse oil-in-water droplets generated through a microfluidics device. The dispersed organic phase consists of MNPs in dichloromethane, and the continuous phase is the aqueous phase of sodium dodecyl sulfate (SDS) and ethylene glycol (PEG) solution. When PEG was added in the aqueous phase, droplets containing MNPs remained a single phase during solvent evaporation. MNPs in the progressively more concentrated solution in the droplets tend to aggregate since the decrease of particle-particle distance causes a great increase of the interparticle interaction including hydrophobic forces, van der Waals forces and magnetic dipole–dipole interaction, giving rise to somewhat clusters after complete removal of organic solvent (b).¹⁰ The results demonstrate that only PEG in oil droplets can produce double emulsions by water diffusion into the preformed single droplets that triggers phase separation. Thus, from the discussion above, the synergy of the combination of PEG, MNPs and the setting temperature during the phase-separated process of droplets, we believe, leads to the formation of the stable and well-defined double emulsions.

References

- (1) Sun, S. H.; Zeng, H. *J. Am. Chem. Soc.* **2002**, *124*, 8204.
- (2) Xie, J.; Xu, C. J.; Kohler, N.; Hou, Y. L.; Sun, S. H. *Adv. Mater.* **2007**, *19*, 3163.
- (3) Zeng, J. F.; Jing, L. H.; Hou, Y.; Jiao, M. X.; Qiao, R. R.; Jia, Q. J.; Liu, C. Y.; Fang, F.; Lei, H.; Gao, M. Y. *Adv. Mater.* **2014**, *26*, 2694.
- (4) Liu, D. F.; Wu, W.; Ling, J. J.; Wen, S.; Gu, N.; Zhang, X. Z. *Adv. Funct. Mater.* **2011**, *21*, 1498.
- (5) Park, J.; An, K.; Hwang, Y.; Park, J. G.; Noh, H. J.; Kim, J. Y.; Park, J. H.; Hwang, N. M.; Hyeon, T. *Nat. Mater.* **2004**, *3*, 891.
- (6) Wei, W.; Yuan, L.; Hu, G.; Wang, L. Y.; Wu, J.; Hu, X.; Su, Z. G.; Ma, G. H. *Adv. Mater.* **2008**, *20*, 2292.
- (7) Jurado-Sánchez, B.; Sattayasamitsathit, S.; Gao, W.; Santos, L.; Fedorak, Y.; Singh, V. V.; Orozco, J.; Galarnyk, M.; Wang, J. *small* **2015**, *11*, 499.
- (8) Ku, K. H.; Shin, J. M.; Kim, M. P.; Lee, C.-H.; Seo, M.-K.; Yi, G.-R.; Jang, S. G.; Kim, B. J. *J. Am. Chem. Soc.* **2014**, *136*, 9982.
- (9) Chen, O.; Riedemann, L.; Etoc, F.; Herrmann, H.; Coppey, M.; Barch, M.; Farrar, C. T.; Zhao, J.; Bruns, O. T.; Wei, H.; Guo, P.; Cui, J.; Jensen, R.; Chen, Y.; Harris, D. K.; Cordero, J. M.; Wang, Z. W.; Jasanoff, A.; Fukumura, D.; Reimer, R.; Dahan, M.; Jain, R. K.; Bawendi, M. G. *Nat. Commun.* **2014**, *5*, 5093.
- (10) Qiu, P. H.; Jensen, C.; Charity, N.; Towner, R.; Mao, C. B. *J. Am. Chem. Soc.* **2010**, *132*, 17724.